

Photocurrent measurements of electric-field-induced carrier energy shifts and tunnelling in  
 $\text{In}_{1-x}\text{Ga}_x\text{As}/\text{InP}$  quantum wells

This article has been downloaded from IOPscience. Please scroll down to see the full text article.

1989 J. Phys.: Condens. Matter 1 2041

(<http://iopscience.iop.org/0953-8984/1/11/012>)

View [the table of contents for this issue](#), or go to the [journal homepage](#) for more

Download details:

IP Address: 171.66.16.90

The article was downloaded on 10/05/2010 at 17:59

Please note that [terms and conditions apply](#).

## Photocurrent measurements of electric-field-induced carrier energy shifts and tunnelling in $\text{In}_{1-x}\text{Ga}_x\text{As}/\text{InP}$ quantum wells

M G Shorthose and J F Ryan

Clarendon Laboratory, Parks Road, Oxford OX1 3PU, UK

Received 14 October 1988

**Abstract.** We have measured photocurrent in  $\text{In}_{1-x}\text{Ga}_x\text{As}/\text{InP}$  quantum well samples as a function of temperature and applied electric field in order to study the escape of carriers initially photo-excited into the wells. For fields of  $8 \times 10^4 \text{ V cm}^{-1}$ , there is suppression of the excitonic features in the spectrum which is attributed to a low exciton ionisation rate which causes carriers to recombine within the well rather than to undergo perpendicular transport. At higher fields, we observe strong Stark shifts of the excitons. We observe clear evidence of carrier tunnelling at low temperatures, and at higher temperatures we detect phonon-assisted tunnelling. The experimental results are shown to be in good agreement with the predictions of an exact theoretical calculation.

Optical studies of semiconductor quantum well structures in the presence of applied electric fields show remarkable properties which are a direct consequence of carrier confinement. Excitonic absorption lines in quantum wells persist up to very high fields ( $\geq 10^5 \text{ V cm}^{-1}$ ), and they shift to a lower energy by substantial amounts ( $\geq 50 \text{ meV}$ ). This form of the Franz–Keldysh effect has been termed the quantum-confined Stark effect [1]. Quenching of the excitonic recombination luminescence is also observed [2]. This is now known to be due to a combination of reduced spatial overlap of the electron and hole wavefunctions, which is important in wide wells [3], and also from carrier tunnelling through the confining barriers, which is more important in narrow wells [4]. Much of the experimental and theoretical effort to date has been devoted to  $\text{GaAs}/\text{Ga}_{1-x}\text{Al}_x\text{As}$  structures [5], but the requirements for devices that operate at longer wavelengths near 1.3 and 1.5  $\mu\text{m}$  has led to increased interest in  $\text{In}_{1-x}\text{Ga}_x\text{As}/\text{InP}$  structures [6, 7]. In this paper we report photocurrent measurements of a single  $\text{In}_{1-x}\text{Ga}_x\text{As}$  quantum well in fields up to  $2.7 \times 10^5 \text{ V cm}^{-1}$  and at temperatures ranging from 5 to 170 K. We compare the experimental results with the results of an exact theoretical calculation which yields field-dependent wavefunctions, energy level shifts and carrier tunnelling times.

The sample we studied was grown by metallo-organic vapour-phase epitaxy as described previously [8]. It consists of a single quantum well of width 110  $\text{\AA}$  grown in the middle of a nominally undoped InP region of width 1  $\mu\text{m}$ , which itself is contained within a p–i–n diode structure [7]. Perpendicular electric fields were then obtained by reverse biasing the diode. Photocurrent is detected when carriers which have been optically excited in the wells escape into the barrier region; to do this, they must surmount a

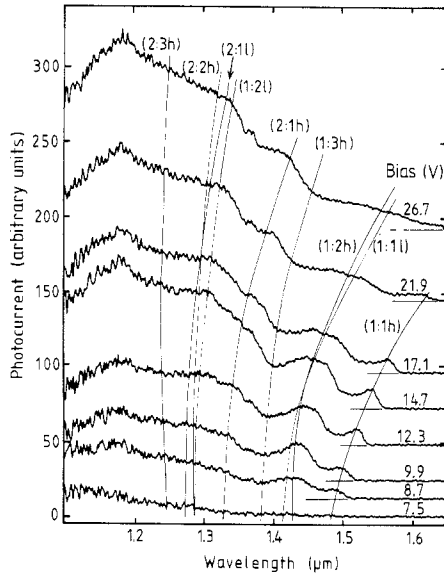


**Figure 1.** Photocurrent spectra obtained from a single  $110 \text{ \AA}$   $\text{In}_{1-x}\text{Ga}_x\text{As}$  quantum well at 80 K as a function of bias voltage: —, theoretical values of the inter-sub-band transition energies obtained from the model described in the text. The spectra have been offset for clarity.

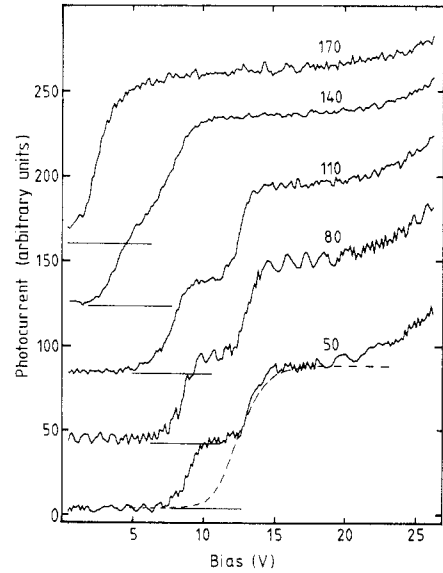


**Figure 2.** Dependence on the temperature (given on traces, in K) of the photocurrent against bias measured for a single  $110 \text{ \AA}$   $\text{In}_{1-x}\text{Ga}_x\text{As}$  quantum well at an excitation wavelength of  $1.2 \text{ \mu m}$ : ---, calculated photocurrent obtained from the electron tunnelling lifetime.

substantial energy barrier and, at low biases, no photocurrent is expected as carriers cannot escape from the wells. As the bias is increased, the internal electric field effectively reduces the width of the barrier so that carriers can escape, and an increase in photocurrent is therefore expected. The single-well configuration was used here as opposed to a multiple-well sample in order to ensure field uniformity.

Figure 1 shows spectra obtained at 80 K for reverse biases between 7.5 and 26.7 V. At the lowest bias the spectrum is flat and featureless. At higher biases, there is a general increase in the magnitude of the photocurrent, indicating that more carriers escape from the well. At 8.7 V, there is clear  $n = 1$  heavy-hole (1:1 h) and light-hole (1:1 l) excitonic structure and, at higher energies,  $n = 2$  transitions become evident. This structure becomes more distinct with increasing bias and is most prominent at biases of about 12–15 V. At higher biases, there is strong shifting of the  $n = 1$  transition, and the excitonic structure broadens substantially.

In figure 1 an additional spectral feature appears between the  $n = 1$  light-hole and the  $n = 2$  heavy-hole excitonic transitions. We attribute this to a normally parity-forbidden (2:1 h) transition from the  $n = 1$  heavy-hole sub-band to the  $n = 2$  electron sub-band [9]. The (1:2 h) transition, although not distinct in figure 1, is probably responsible for the rapid spectral broadening in the region of the  $n = 1$  light-hole exciton. Similarly the (1:2 l) and the (2:1 l) transitions may cause broadening of the (2:2 h) absorption edge. There is also a feature in figure 1 at  $1.176 \text{ \mu m}$  that shifts very little but which becomes stronger with increasing field. This transition is possibly from the  $n = 1$  heavy valence band to continuum states above the conduction band well [10].

In figure 2, we present measurements of photocurrent against bias for an incident light wavelength of  $1.20 \text{ \mu m}$  and sample temperatures between 50 and 170 K. At low

temperatures a bias of about 8 V is required before a sizeable photocurrent is detected. For bias 8 V there is a sharp increase in photocurrent followed by levelling out at 10 V. At 12 V, there is another increase in photocurrent, followed by levelling out at 15 V. At higher temperatures, a lower bias is required for initial detection of photocurrent and, above about 160 K, only a single plateau is observed. This structure in the field dependence of the photocurrent is explained below in terms of competing dynamical processes: exciton formation, dissociation and recombination, and carrier escape from the well including tunnelling.

Theoretical calculations of the energies of the Stark resonances in this problem have employed a variety of approximate [11] and exact methods [12]. We have used an **R** matrix method [13] which avoids approximations leading to inaccuracies at high fields, and which yields the tunnelling rates of the carriers through the confining barrier. In the effective-mass approximation the Schrödinger equation for motion along  $z$  is

$$-\left(\hbar^2/2m_b\right)(d^2/dz^2)\Psi + (V_o + eFz)\Psi = E\Psi \quad |z| > L/2 \quad (1a)$$

$$-\left(\hbar^2/2m_w\right)(d^2/dz^2)\Psi + eFz\Psi = E\Psi \quad |z| \leq L/2 \quad (1b)$$

where  $\Psi$  is the particle envelope function,  $m_w$  and  $m_b$  are the effective masses in the well and barrier, respectively,  $V_o$  is the band offset and  $F$  is the electric field. Boundary conditions on the continuity of  $\Psi$  and particle flux at the well-barrier interfaces at  $z = \pm L/2$  are applied. On the high-potential side of the well,  $\Psi$  decays into the barrier whereas, on the low-potential side,  $\Psi$  is a propagating function giving rise to a non-zero flux.

The general solutions of (1) are of the form of the Airy functions  $A_i, B_i$ :

$$\Psi_1 = a_1[B_i(\eta_b) + iA_i(\eta_b)] \quad z < L/2 \quad (2a)$$

$$\Psi_2 = a_2A_i(\eta_w) + b_2B_i(\eta_w) \quad -L/2 < z < L/2 \quad (2b)$$

$$\Psi_3 = a_3A_i(\eta_w) \quad z > L/2 \quad (2c)$$

where

$$\eta_b = -[2m_b/e\hbar F]^2(E - V_o - eFz) \quad (3a)$$

$$\eta_b = -[2m_w/(e\hbar F)^2]^2(E - eFz). \quad (3b)$$

In [14], solutions were obtained by solving the secular determinant. We have chosen the **R**-matrix method mainly because of its computational simplicity, but also because it can be easily extended to the case of multiple-well structures which are also of interest. The **R** matrix is defined by

$$\Psi = \mathbf{R} d\Psi/dz. \quad (4)$$

**R** is readily evaluated using the boundary condition on the outgoing wave, and by using propagation rules it can be determined at all points within the structure. The resonance energies are then obtained from the zeros of the **S** matrix in the region  $z > L/2$ :

$$\mathbf{S} = (\mathbf{R} dA_i/d\eta - A_i)/(\mathbf{R} dB_i/d\eta - B_i). \quad (5)$$

We have adapted the method in [13] to allow the **S** matrix to be minimised with respect to energy in the complex energy plane. The resulting energies are complex:

$$E = E_o - i\Gamma/2 \quad (6)$$

and the tunnelling rate is given by  $\hbar/\Gamma$ .

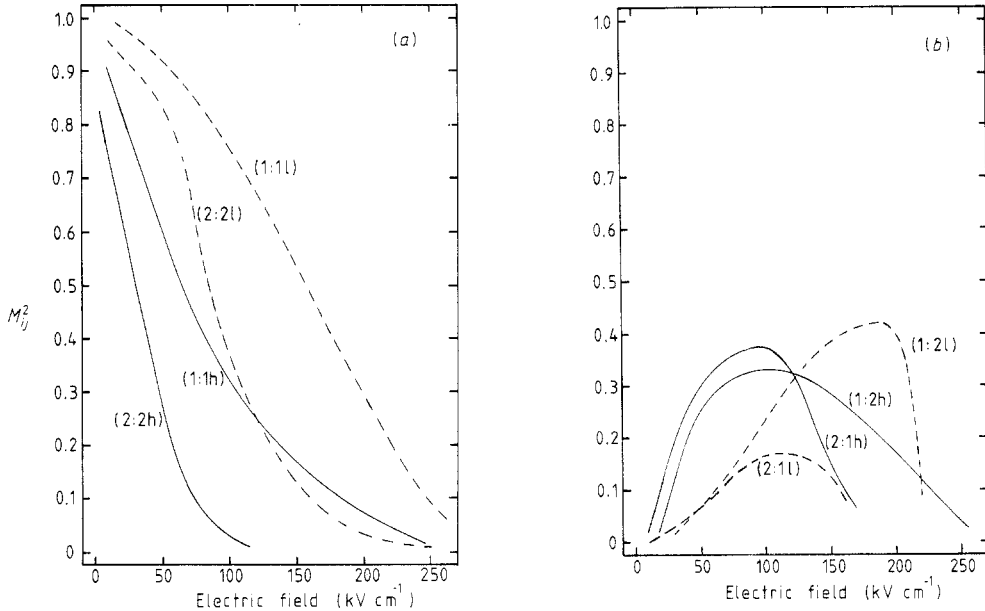


**Figure 3.** Calculated values of the oscillator strengths of inter-band transitions in presence of an applied electric field: (a) 'allowed' transitions; (b) normally 'parity-forbidden' transitions.

The model thus far is exact but, in applying it to the problem at hand, we have made several simplifying assumptions. The bands are assumed to be parabolic and isotropic, and mixing of light- and heavy-hole states in the presence of an electric field is neglected. Furthermore, we limit the calculation to that of the sub-band energies. Excitonic effects are not considered, although it would be straightforward to include them as perturbations; the justification for this is that exciton binding energies are much less susceptible to applied electric fields than are the band states themselves [11]. We have used this model to calculate the shift of  $n = 1$  and  $n = 2$  optical transitions using an  $\text{In}_{0.53}\text{Ga}_{0.47}\text{As}$  band gap of 816 meV and conduction and valence band offsets of 250 meV and 375 meV, respectively. We use electron masses  $m_w^e = 0.041 m_0$  and  $m_b^e = 0.08 m_0$ , heavy-hole masses  $m_w^h = 0.5 m_0$  and  $m_b^h = 0.56 m_0$ , and light-hole masses  $m_w^l = 0.051 m_0$  and  $m_b^l = 0.12 m_0$ . We made corrections for non-parabolicity in the electron and light-hole bands by using the standard expression  $m^* = m(1 + \kappa E/E_G)$  with  $\kappa = 1.6$  [8]. The results of the calculation are shown in figure 1. We find excellent agreement between theory and experiment if external bias  $V$  and internal field  $E$  are related via  $F = V/D$ , where the effective intrinsic region length  $D$  is 1  $\mu\text{m}$ .

The calculated oscillator strengths for the (band-to-band) transitions

$$M_{ij}^2 = \left| \int \Psi_e \Psi_v dz \right|^2 \quad (7)$$

are shown in figure 3. The (1:1) heavy-hole–electron and light-hole–electron transition strengths decrease with increasing field as expected on the basis of previous calculations [9]. The (2:2) transitions decrease more rapidly than the (1:1) transitions because the wavefunctions of the former are already extended towards the interfaces in zero field. The (2:1h) and (1:2l) transitions, on the contrary, increase rapidly in strength with

increasing field; at  $2 \times 10^5 \text{ V cm}^{-1}$  the (1:2 1) transition is the strongest, which is consistent with the assignment of this feature in figure 1. The (2:1 h) transition, however, is not observed to decay as rapidly as predicted at high fields. It is also clear from figure 3 that the (1:2 h)/(1:1 1) and (2:2 h)/(2:1 1) pairs of transitions show a level crossing. In a more realistic model where mixing of the hole states is permitted, a level repulsion would result.

Comparing figures 1 and 2, we see that the  $n = 1$  exciton features become apparent only above the lower threshold bias voltage. Although we have been unable to measure optical absorption in the single wells in applied fields we have studied a multiple-well sample; at low biases, we observe sharp excitonic structure in absorption, and also strong excitonic photoluminescence [8]. From this evidence, we conclude that, for low biases, photo-excited carriers relax rapidly to form excitons and subsequently to recombine. Under these conditions there is very little photocurrent. With increasing bias and/or temperature, excitons dissociate more readily and carriers can escape from the well. However, our calculation shows that the tunnelling rate is very small for biases of less than 10 V and so contributes very little to the photocurrent. For biases between 10 V and 15 V the tunnelling lifetime for electrons is calculated to decrease from 11 ns to 28 ps; electrons begin to escape from the well more quickly than they can recombine within the well and so the photocurrent increases. The current produced at a given bias and illumination intensity depends on the rate of exciton formation and dissociation and also on the ratio of the tunnelling to recombination rates. A rate equation analysis of the electron dynamics yields the following phenomenological expression for the current:

$$I = I_0(1 + \alpha\hbar/\Gamma)^{-1}. \quad (8)$$

In the limit of rapid exciton dissociation,  $\alpha$  is given by the recombination rate multiplied by the ratio of the exciton formation to exciton dissociation rates. The calculated photocurrent for  $\alpha = 3 \text{ ns}^{-1}$  is shown by the broken line in figure 2; it shows a strong increase at biases higher than 10 V, in good agreement with the experimental results. The current reaches a plateau when all electrons photo-excited in the wells escape by tunnelling. For biases greater than 20 V, the photocurrent shows a slow increase owing probably to the onset of tunnelling from hole states in the well.

The low-bias threshold for the onset of photocurrent cannot be explained by direct carrier tunnelling. The high quality of the InP barriers together with the observed decrease in bias threshold with increasing temperature rule out impurity-related processes. Preliminary calculations show that this effect is due to phonon-assisted tunnelling in which electrons interacting with longitudinal optical phonons are excited to higher-energy states within the well for which the tunnelling lifetime is relatively short. Details of this calculation will be published elsewhere.

In conclusion we have measured Stark shifts of confined excitons in  $\text{In}_{1-x}\text{Ga}_x\text{As}$  quantum wells and find good agreement with theoretical calculations for fields up to  $2.5 \times 10^5 \text{ V cm}^{-1}$ . The theoretical tunnelling rate accounts well for the observed increase in photocurrent at high fields. A large temperature-dependent photocurrent observed at low fields is assigned to phonon-assisted tunnelling of electrons from the well.

### Acknowledgments

We wish to thank M D Scott, J I Davies and A Moseley (Plessey, Caswell) who supplied the sample.

**References**

- [1] Miller D A B, Chemla D S, Damen T C, Gossard A C, Wiegmann W, Wood T H and Burrus C A 1984 *Phys. Rev. Lett.* **53** 2173
- [2] Mendez E E, Bastard G, Chang L L and Esaki L 1982 *Phys. Rev. B* **26** 7101
- [3] Polland H-J, Schultheis L, Kuhl J, Göbel E O and Tu C W 1985 *Phys. Rev. Lett.* **55** 2610
- [4] Kash J A, Mendez E E and Morkoc H 1985 *Appl. Phys. Lett.* **46** 173
- [5] Miller D A B, Chemla D S, Damen T C, Gossard A C, Wiegmann W, Wood T H and Burrus C A 1985 *Phys. Rev. B* **32** 1043
- [6] Bar-Joseph I, Klingshirn C, Miller D A B, Chemla D S, Koren U and Miller B I 1987 *Appl. Phys. Lett.* **50** 1010
- [7] Shorthose M G, Maciel A C, Ryan J F, Scott M D, Moseley A, Davies J I and Riffat J R 1987 *Appl. Phys. Lett.* **51** 493
- [8] Shorthose M G, Maciel A C, Ryan J F, Scott M D, Davies J I and Moseley A 1988 *Semicond. Sci. Technol.* **3** 616
- [9] Ikonić Z, Milanović V and Tjapkin D 1987 *J. Phys. C: Solid State Phys.* **20** L425
- [10] Skolnik M S, Tapster P R, Bass S J, Pitt A D, Apsley N and Aldred S P 1986 *Semicond. Sci. Technol.* **1** 29
- [11] Bastard G, Mendez E E, Chang L L and Esaki L 1983 *Phys. Rev. B* **28** 3241
- [12] Austin E J and Jaros M 1985 *J. Phys. C: Solid State Phys.* **18** L1091
- [13] Schwartz C 1987 *Appl. Phys. Lett.* **50** 457
- [14] Ahn D and Chuang S L 1986 *Phys. Rev. B* **34** 9034